DOI 10.1007/s10812-018-0717-2
Journal of Applied Spectroscopy, Vol. 85, No. 4, September, 2018 (Russian Original Vol. 85, No. 4, July–August, 2018)

EARLY STAGE DETECTION OF STRESS DUE TO COPPER ON MAIZE (*Zea mays L.)* BY LASER-INDUCED FLUORESCENCE AND INFRARED SPECTROSCOPY

S. Sharma and K. N. Uttam*

UDC 535.372.535.34

Laser-induced fluorescence (LIF) and attenuated total reflectance Fourier transform infrared (ATR-FTIR) spectroscopy has been applied for the nondestructive, label free, and rapid analyses of the impact of copper (25, 50, and 75 μM) on maize seedlings at an early stage before the changes appear visually on the plant. The LIF measurement has been used to detect the signs of stress in the photosynthetic pigment. The integrated areal intensity and increasing fluorescence intensity ratios indicate decrease in the photosynthetic pigments in the leaves of maize plants stressed with copper. The ATR-FTIR technique has been utilized to estimate the changes arising in the cell wall polysaccharides, amino acid, secondary structure of protein and lipid content of the leaves of control and copper-treated maize seedlings. The second derivative and curve fitting analyses have been applied for the enhancement of the spectral variations and quantitative estimation of the changes arising in the biochemical profile. The result shows an increase in the pectin, lignin, amino acid, and protein content and reduction in the amount of cellulose and lipid in the leaves of maize seedlings due to the treatment of copper. This study indicates the toxic response of copper by hampering the growth and reduction in the photosynthetic pigments and biochemical content of the maize seedlings. This study also demonstrates the feasibility of the spectroscopic techniques (LIF and ATR-FTIR) as a rapid, label free, and nondestructive probe for the assessment of stress and monitoring of crops.

Keywords: *laser-induced fluorescence spectroscopy, attenuated total reflectance Fourier transform infrared spectroscopy, biochemical analysis, curve fitting analysis, heavy metal stress.*

Introduction. Maize (*Zea mays L.*) belongs to the Maydeae group of the Poaceae family, and its plants have been used since long as fodder for animals while maize grains are used as food by human [1]. Copper is required by the plants as an essential micronutrient and is involved in metabolic processes like photosynthesis and respiratory electron transport chain. It also acts as a cofactor of various key enzymes that are involved in metabolic processes, including ATP synthesis [2]. Copper is introduced into agricultural soil through anthropogenic activities such as extensive use of pesticides and application of sewage, sludge, mining, and smelting activities associated with copper. Copper is mainly absorbed as Cu^{2+}, and the excess absorbed copper is considered toxic as it causes a range of morphological and physiological changes inside the plant. Copper in excess is known to reduce leaf area, overall growth of plant, and alter photosynthetic activity [3–5]. The application of copper to wheat (*Triticum aestivum L.*) seedlings significantly decreases the chlorophyll content but elevates the H_2O_2 and MDA contents, as well as stimulates the activities of superoxide dismutase, peroxidase, and catalase enzymes [6]. An excess copper (Cu^{2+}) exposure on *Salix purpurea* also increases the accumulation of soluble carbohydrates and phenolics, including salicylic acid and glutathione, in *Salix* leaves [4]. Copper adversely affects nitrogen metabolism by decreasing nitrate reductase activity in roots and shoots of the *Brassica pekinensis Rupr.*, while it increases total free amino acids in the leaves [7]. The application of copper to *Vigna mungo L.* seedlings reduces the chlorophyll, sugar, and carotenoid contents, but it increases the proline and total phenolic contents by stimulating the activity of antioxidant enzymes (peroxidase, polyphenol oxidase, catalase, and superoxide dismutase) [8]. Plants of *Pinus sylvestris L.* grown on a copper-contaminated site show significant growth inhibition in dwarf shoots and whole needles with increase in water content and reduced dry mass. The exposure also increases the electrolyte leakage and rate of respiration in needles of the plants [9]. The plants of Indian Jinxing

*To whom correspondence should be addressed.

University of Allahabad, Allahabad, India; e-mail: kailash.uttam@rediffmail.com. Abstract of article is published in Zhurnal Prikladnoi Spektroskopii, Vol. 85, No. 4, p. 684, July–August, 2018.

show toxic effects of copper, which is reflected by the reduction in chlorophyll content, carotenoids content, and growth of the plant. The level of hydrogen peroxide (H_2O_2) and superoxide anions ($O_2^{\bullet -}$) is also higher in the treated plants [10]. Chronic exposure of copper to Scots pine (*Pinus sylvestris L.*) leads to loss in dominance of the main root with the inhibition of lateral root development and interference with the absorption of iron and manganese [11].

With increase in the level of heavy metal stress in vegetation, analytical techniques are required that can detect the changes or damages prior to the appearance of signs of visual toxicity. Techniques available for the plant diagnosis are largely based on chemical methods and are destructive to the plant tissue samples. The chemical method involves extraction of the desired compounds in a solvent matrix, which changes the configuration of molecules, and is influenced by the type of molecule under consideration, chemical nature of the extracting solvent, and process involved in the diffusion of compound into the solvent matrix. Spectroscopy techniques can be successfully applied to study the physiological and metabolic status of plants under stress condition without the destruction and extraction of the sample involved. Spectroscopic techniques like LIF and ATR-FTIR have emerged as nondestructive and noninvasive molecular identification techniques that have rapid data collection capability and are sensitive probes to detect even minor alterations in the surrounding conditions. Laser-induced chlorophyll fluorescence is a potential technique to investigate plant physiology and plant stress. The light-induced chlorophyll fluorescence of plant tissues provides information on functioning of the photosynthetic apparatus. The fluorescence parameters (peak area, peak width, and peak intensity) obtained after Gaussian curve fitting are strongly affected by the various environmental stress factors. The fluorescence intensity ratio is also a useful indicator of the amount of chlorophyll present in the leaf [12]. The advantage of measuring different parameters of chlorophyll fluorescence using LIF is that it provides rapid information on photosynthetic performance. In addition, it is a sensitive, nondestructive technique and can be used in vivo on very small amounts of sample.

Infrared spectroscopy is a powerful technique for the determination of molecular vibrations that correspond to a specific functional group. The structure of biological compounds or its functional groups can be probed through FTIR spectroscopy and offers a fast method to fingerprint the chemicals under specific condition. By analyzing the position, intensity, width, and area of the acquired spectra, changes in composition and conformation arising in the biological system due to the changing environment can be detected [13–15]. With the development of a wide range of sampling accessories like an ATR unit, sample handling has become user friendly. The ATR unit minimizes the need for sample preparation and is able to detect molecular changes with high sensitivity the changes by rapid acquisition of the spectrum from a very small amount of sample.

Sometimes, due to the low resolving power of the instrument, the infrared bands lie at very close proximity and overlap with each other. Consequently, they form a broad band that becomes relatively featureless. The second derivative is a commonly used process of spectral analyses that allows extracting appropriate information on weak bands and component bands, increases the specificity of the infrared bands, reduces replicate variability, and removes constant and linear components of the baseline; hence it can be used to amplify spectral variations by increasing the number of discriminative features. The method of curve fitting allows reconstructing an original spectrum or a part of it using a set of bands in order to uncover the bands that are underlie the broad bands. Curve fitting of the bands narrows down the width of the overlapping component bands and separates them beyond the resolving power of the instruments.

A review of the existing literature reveals that the information available on copper stress on the maize plants is inadequate to describe its effects in the early stage of the seedling growth until the visual sign of toxicity appears on the plants. Most of the techniques available to study these effects are based on chemical methods that involve time consuming, labor intensive, and complex procedures of extraction and treatment. Thus, the present study describes an alternate approach for plant diagnosis based on spectroscopic markers of biochemical and curve fitting that are free from calibration, chemical treatment, and extraction. It describes the potential of LIF and ATR-FTIR spectroscopy as nondestructive, rapid, and sensitive techniques of plant stress diagnostics. The stress response shown by maize seedlings towards copper at different concentrations (25, 50, and 75 μM) in terms of biochemical content such as chlorophyll, carotenoid, cellulose, pectin, lignin, amide II, amide I, and lipid has been accessed. The change in chlorophyll content is observed using the laser-induced fluorescence technique, while variations in the cellulose, pectin, lignin, amide I, amide II, and lipid have been evaluated by ATR-FTIR spectroscopy.

Materials and Methods. *Plant material and growth conditions.* The growth and development conditions, in addition to the experimental procedure, is described elsewhere [13]. Briefly, all the chemicals were obtained from commercial suppliers and used as received with no further treatment. The seeds of maize were procured from the local seed market of Allahabad, India. Uniform sized seeds were sorted, surface sterilized in 4% NaClO solution for 20 min, washed with distilled water, and transferred on a wet filter paper placed in a Petri dish and kept in the dark for 4 days at 28 ± 2°C. Uniformly germinated seeds

were transferred to plastic pots containing acid washed sand and were grown on Hoagland nutrient solution. Seedlings were grown under a control photosynthetic photon flux density and relative humidity. Then after 6 days of the growth, a copper treatment was given to the seedlings through roots in the sand matrix at different concentrations (25, 50, and 75 μM) in the form of the $CuSO_4 \cdot 5H_2O$ in 1/4 strength Hoagland medium. Copper toxicity was introduced into the seedlings on alternate days. After 9 days of treatment, the second leaves of the plants were used for the spectroscopic observations. Seedlings grown on the Hoagland medium without toxicity were regarded as control seedlings.

After harvesting the control and copper-treated plants, the growth and biomass parameters like length of shoot, fresh weight of shoot, and dry weight of shoot were determined.

Estimation of pigments using LIF and UV-Vis spectroscopy. The LIF spectra of the leaves of the adaxial surface of the control and copper-treated maize seedlings were recorded using a 405 nm violet diode laser of 50 mW power (Oxxius CE, model PS-007) as an excitation source. The emitted fluorescence was recorded using a 600 μm optical fiber attached to a fiber optic spectrometer (Avantee, Ava-Soft-3648, Netherlands). The spectra were recorded in the spectral region of 400–800 nm at a resolution of 2.3 nm. The band parameters (band area, width, and height) and fluorescence intensity ratio of the obtained bands were calculated from the fitted curve for which fitting of the bands was performed using an Origin 8.0 package.

For the quantification of chlorophyll *a*, chlorophyll *b*, and carotenoids, 100 mg fresh leaves from the control and copper-treated seedlings were cut into small pieces and crushed in 80% acetone and 20% distilled water (80%, v/v). The extracts were centrifuged at 6000 rpm for 10 min. The UV-Vis spectra of the extracts were recorded in the spectral region of 200–800 nm using a fiber optic spectrometer (Avantee, Ava-Soft-3648, Netherlands) at a resolution of 2.3 nm. The obtained absorbance values were used for the estimation of pigments. The absorbance value of the chlorophyll *a* band at 663.2-nm, chlorophyll *b* at 646.5-nm, and caraotenoids (Car) detected at 470-nm wavelength was used for estimating the content of the pigments. The amount of chlorophylls (Chl *a* and Chl *b*) and carotenoids was estimated using Lichtenthaler's equations (1987) [16]

$$\text{Chl } a \text{ (μg/mL)} = 12.25(A_{663.2}) - 2.79(A_{646.5}) ,$$

$$\text{Chl } b \text{ (μg/mL)} = 21.50(A_{646.5}) - 5.10(A_{663:2}) ,$$

$$\text{Car (μg/mL)} = [(1000A_{470} - 1.82(\text{Chl } a) - 85.02(\text{Chl } b)]/198 .$$

ATR-FTIR measurement for the analysis of biochemicals. The ATR-FTIR measurements on the adaxial surface of leaves of the control and copper-treated maize seedlings were performed on an ABB Bomem FTIR MB 3000 spectrometer (ABB Analytical Measurements, Canada) equipped with a Pike miracle ATR unit in the spectral region of 4000–485 cm^{-1} at a resolution of 4 cm^{-1}. The leaves were scanned at a distance of 4 cm above the node and at 4 adjacent positions. In order to improve the signal-to-noise ratio, 25 scans were collected, and the resultant average intensity was analyzed. The spectra were smoothed by the Savitzky–Golay method in a polynomial window of 9 points with a 21-point moving window. The second derivative of the spectral profile was generated using Horizon MB^{TM} FTIR processing software to determine the positions of the band components clearly for the curve fitting of the bands. The curve fitting of the band was performed using Origin 8.0 package for the estimation of area of the band that was used for the quantitative assessment of the changes in cell wall polysaccharides, protein secondary structure, and lipid. A Gaussian shape was used for fitting the recorded infrared bands. The accuracy of the curve fitting was determined by fit standard errors.

Statistical analyses. The reproducibility of the results was checked by performing three independent experiments with three replicates in each experiment. The experimental results were subjected to analysis of variance (ANOVA) using SPSS 20.0 software for Windows. The data were reproduced in the form of mean ± standard error of three independent experiments with three replicates in each experiment. The Tukey's multiple range test at the 5% significance level was used for the comparison of means, and the resultant honesty significance difference (HSD) was reported with different characters.

Results and Discussion. The growth and biomass parameters like shoot length, fresh weight, and dry weight showed continuous retardation upon treatment with copper and is presented in Table 1. The tabulated data have been presented as mean ± standard error at a significance level of $P < 0.05$. The significance level of the tabulated values amongst each other has been denoted by different alphabet. The shoot length was reduced by 19.41, 20.95, and 28.63%, while fresh weight was reduced by 3.69, 16.26, and 19.93%. The decrease in dry weight was found to be 19.39, 32.07, and 40.35% for the 25, 50, and 75 μM concentration of copper, respectively.

Figure 1 shows recorded steady-state LIF spectrum of the adaxial surface leaf of the control and copper-treated maize plants. The spectrum includes two chlorophyll bands, one in the red region at 685 nm and the other in the far red region

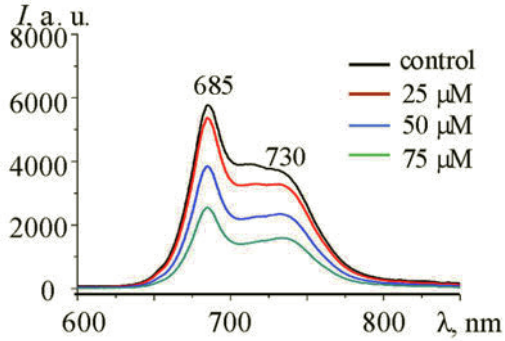

Fig. 1. Laser-induced fluorescence spectra of the control and copper-treated maize (*Zea mays L.*) seedlings excited by a 405-nm diode laser.

TABLE 1. Effect of the Copper on the Growth and Biomass of Maize Seedlings

C_{Cu}, μM	Shoot height, cm	Fresh weight, g	Dry weight, g
Control	39.63 ± 0.010a	1.40 ± 0.040a	0.19 ± 0.002a
25	27.45 ± 0.005b	1.28 ± 0.020b	0.15 ± 0.001b
50	25.47 ± 0.007bc	1.14 ± 0.020c	0.13 ± 0.001c
75	24.07 ± 0.004d	1.03 ± 0.010d	0.11 ± 0.002d

TABLE 2. Impact of Copper Treatment on Chlorophyll *a*, Chlorophyll *b*, Total Chlorophyll, and Carotenoid Content of Maize Seedlings

C_{Cu}, μM	Chlorophyll *a*, mg/g fresh weight	Chlorophyll *b*, mg/g fresh weight	Total chlorophyll, mg/g fresh weight	Carotenoid, mg/g fresh weight
Control	19.03 ± 0.18a	6.28 ± 0.16a	25.31 ± 0.29a	3.44 ± 0.12a
25	14.11 ± 0.04b	4.46 ± 0.067b	18.57 ± 0.08b	2.88 ± 0.03b
50	10.14 ± 0.14c	3.31 ± 0.10c	13.46 ± 0.17c	2.49 ± 0.09c
75	9.87 ± 0.18c	2.49 ± 0.11d	12.37 ± 0.22d	2.49 ± 0.07c

at 730 nm [17]. The chlorophyll fluorescence intensity and area of both the red region and far red region bands decreased in the leaves of the maize seedlings treated with copper. The area of the 685-nm band was decreased by 9.56, 20.35, and 39.50% in leaves of the copper-treated plants. The decrease was more pronounced for the 730 nm band. The decrease was 19.54, 47.79, and 66.93% with respect to the control plants. The fluorescence intensity ratio of the chlorophyll bands 685 and 730 nm (I_{685}/I_{730}) for the control plant was 0.93, while for 25, 50, 75 μM copper concentration, the fluorescence intensity ratios were 1.05, 1.28, and 1.35, respectively.

The recorded UV-VIS spectrum of the extract of leaves of control and copper-treated seedlings showed the presence of the chlorophyll *a* band at 663.2 nm and chlorophyll *b* at 646.5 nm, while the caraotenoid (Car) band was detected at 470 nm. The determined chlorophyll content in the leaves of the maize plants (control and copper-treated) is given in Table 2. The data showed that the copper treatment reduced the chlorophyll content by 26.61, 46.81, and 51.13%, while the reduction in the carotenoid content was 16.21, 27.38, and 27.42% for 25, 50, and 75 μM.

Infrared spectroscopy is an efficient tool to get information on the content and conformation of cell wall components, proteins, and lipids in the plants and the effect of the surrounding environment on their configuration [13]. The recorded infrared spectra of the leaves of the control and copper-treated maize seedlings are shown in Fig. 2a.

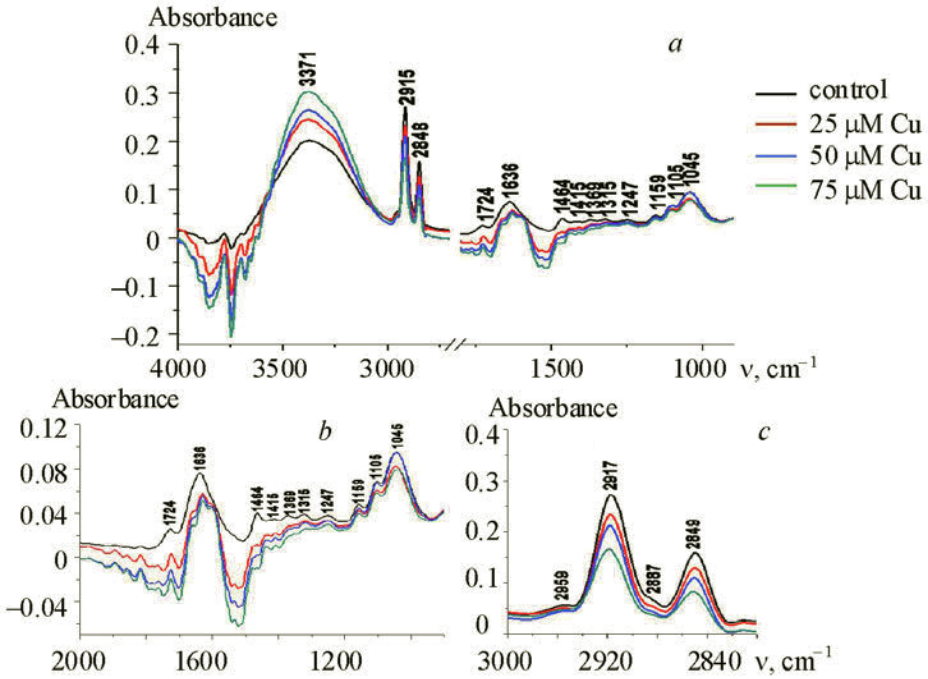

Fig. 2. Recorded (a) and resolution-enhanced infrared spectra in the region of 2000–900 (b) and 3000–2800 cm^{-1} (c) of the leaves of maize seedlings pretreated with copper at different concentrations.

Analyses of the infrared spectrum in the spectral region of 1500–800 cm^{-1}. The fingerprint region of cell wall carbohydrates lies in the spectral region of 1500–800 cm^{-1}. Figure 2b illustrates the recorded spectra of the carbohydrate and lignin present in the leaves of the control and copper-treated maize seedlings. The recorded spectrum consists of absorption bands of cellulose, hemicelluloses, pectin, and phenolic compounds like lignin. The band at 1045 cm^{-1} is due to C–OH bending of arabinoxylans [18]. The absorption band at 1105 cm^{-1} was due to the ν(C–O), ν(C–C), and δ(OCH) ring, and it was assigned to pectin, while the band appearing at 1160 cm^{-1} was attributed to the glycosidic linkage ν(C–O–C) of cellulose [19]. The area of the band at 1107 cm^{-1} increased by 7, 27, and 31%, while the area of the band at 1160 cm^{-1} decreased by 9, 5, and 4% in the leaves of copper treated plants. The deformation of C–O–H and the asymmetric stretch C–O–C of esters were observed at 1247 cm^{-1}, depicted hemicellulose of maize leaves [20]. The CH_2 rocking vibration of cellulose was seen at 1315 cm^{-1} [21], and the area of this band decreased by 40% with respect to the control at all copper exposures. The second derivative of the recorded infrared spectra lying in the region of 1300–1500 cm^{-1} is shown in Fig. 3a. The absorption of pectin due to $\delta_s(CH_2)$ and ν(C–C) [17] was seen at 1368 cm^{-1}, and the area of this band increased by 7, 49, and 53% in the leaves of the copper-treated plants. The C–H deformation of lignin was observed at 1425 cm^{-1} [22], while the band at 1443 cm^{-1} arose due to δ(CH) of pectin [19]. The bands at 1443 and 1480 cm^{-1} were detected in the infrared spectra of the copper-treated leaves of the maize seedlings only, and their area increased with increasing exposure of copper to the plants. The effect of copper on the integrated area of the cell wall polysaccharide bands is given in Table 3. A significantly large increase in the area of the 1425 cm^{-1} band was observed in leaves of the copper-treated plants. These facts indicate modification in the cell wall components in the copper-treated seedlings.

Analyses of the infrared spectrum in the spectral region of 1700–1500 cm^{-1}. The protein component in the maize leaves was represented by two regions: 1600–1500 and 1700–1600 cm^{-1}. The spectral region between 1600–1500 cm^{-1} is characteristic of the amide II bands, while 1700–1600 cm^{-1} is a representative of the amide I bands of protein [13]. The combination of inplane bend of N–H and stretching vibration of the C–N moiety of amide II is represented by the band at 1530 cm^{-1} [23]. When the maize seedlings were treated with copper, the area under the amide II band increased four times with increasing concentration of copper. The amide I band arises at 1635 cm^{-1} and gives an overview on the secondary structure of the protein. The coupling of the C=O stretching vibration of the amide group with in-plane N–H bending generate the ami-de I band [24]. The curve fitting of the amide I band yielded three components at 1601, 1630, and 1660 cm^{-1}. The

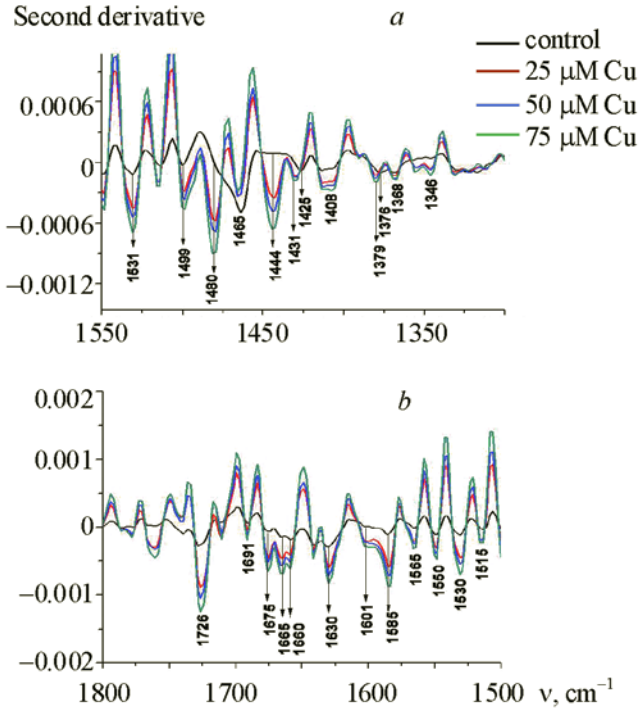

Fig. 3. Second derivative of the recorded infrared spectra of maize seedlings in the region of 1500–1330 (a) and 1800–1550 cm^{-1} (b).

TABLE 3. Band Area of the Spectral Region of 1000–1400 cm^{-1} of the Recorded Infrared Spectrum of the Leaves of the Control and Copper-Treated Maize Seedlings

C_{Cu}, μM	1107 cm^{-1}	1160 cm^{-1}	1319 cm^{-1}	1368 cm^{-1}	1425 cm^{-1}	1443 cm^{-1}	1480 cm^{-1}
Control	0.25 ± 0.01a	0.25 ± 0.00ab	0.14 ± 0.01a	0.10 ± 0.00a	0.04 ± 0.02a	–	–
25	0.27 ± 0.01ab	0.23 ± 0.01c	0.08 ± 0.01b	0.11 ± 0.01a	0.08 ± 0.01a	0.13 ± 0.02a	0.36 ± 0.02a
50	0.31 ± 0.02bc	0.24 ± 0.00bc	0.08 ± 0.00b	0.16 ± 0.01b	0.10 ± 0.03ab	0.17 ± 0.01a	0.43 ± 0.02ab
75	0.33 ± 0.01c	0.26 ± 0.01ab	0.08 ± 0.01b	0.16 ± 0.01b	0.17 ± 0.02b	0.26 ± 0.02b	0.51 ± 0.01b

TABLE 4. Band Area of the Spectral Region of 1500–1700 cm^{-1} of the Recorded Infrared Spectrum of the Leaves of the Control and Copper Treated Maize Seedlings

C_{Cu}, μM	1594–1609 cm^{-1}	1630–1635 cm^{-1}	1659–1665 cm^{-1}
Control	1.12 ± 0.18a	1.52 ± 0.10a	1.69 ± 0.06a
25	2.25 ± 0.11b	2.11 ± 0.15b	1.77 ± 0.10a
50	3.26 ± 0.15c	2.22 ± 0.06b	2.43 ± 0.11b
75	3.87 ± 0.12d	2.58 ±0.06c	2.82 ± 0.07c

second derivative and fitted curves of the amide bands are shown in Figs. 3b and 4. The absorption peak at 1601 cm^{-1} indicates the presence of side chain absorption, and this band is attributed to the vibration (phenyl) of tyrosine [25]. There was an enormous increase in the area of this band in the spectra of the copper-treated leaves. The amide band at 1630 cm^{-1} corresponded to the β-sheet of protein, while the band at 1660 cm^{-1} was assigned to the α-helix structure of amide I band

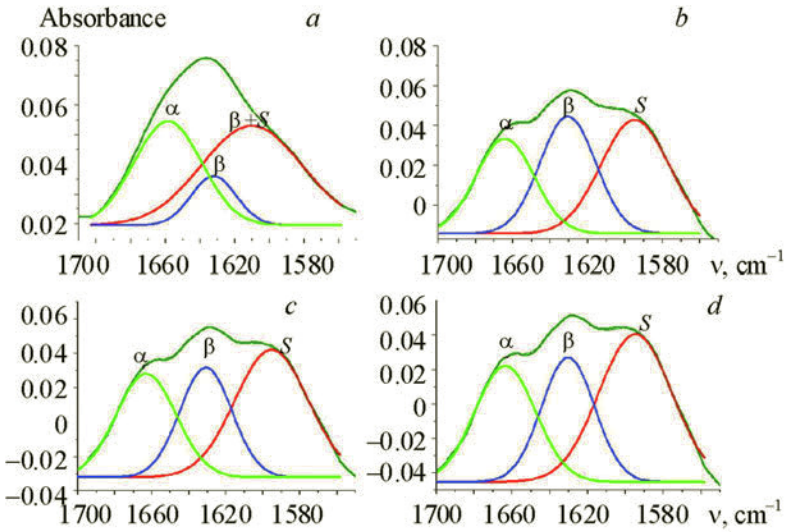

Fig. 4. Curve-fitted spectra of the amide I region (1700–1500 cm^{-1}) of maize seedlings treated with copper at concentrations (a) control, (b) 25 μM, (c) 50 μM, and (d) 75 μM; S, α, and β indicate side chain, α-helical, and β-sheet respectively.

TABLE 5. Band Area of the Spectral Region of 2800–3000 cm^{-1} of the Recorded Infrared Spectrum of the Leaves of the Control and Copper-Treated Maize Seedlings

C_{Cu}, μM	2849 cm^{-1}	2917 cm^{-1}	2959 cm^{-1}	A_{2917}/A_{2959}
Control	3.75 ± 0.08a	7.26 ± 0.19ac	0.39 ± 0.10a	19.89 ± 0.87a
25	2.68 ± 0.06a	5.76 ± 0.74b	0.27 ± 0.04b	17.77 ± 0.39a
50	2.02 ± 0.13b	4.66 ± 0.02c	0.25 ± 0.06b	14.39 ± 0.51b
75	1.63 ± 0.03b	3.85 ±.07d	0.23 ± 0.02b	8.89 ± 0.48c

[25]. The effect of copper on the area of these bands is displayed in Table 4. The area of the β-sheet continuously increased by 38.81, 6.05, and 69.73% in the leaves of the copper-treated maize seedlings. Also the area of the α-helix band component showed a slight increase of 4.73% for 25 μM copper treatment, while treatments with 50 and 75 μM copper increased the peak area by 43.78 and 66.86%, respectively.

Analyses of the infrared spectrum in the spectral region of 3000–2800 cm^{-1}. The lipid content of the leaf was represented by the molecular fingerprint region of 3000–2800 cm^{-1} [13] and is shown in Fig. 2c. The strong bands at 2850 and 2917 cm^{-1} are due to symmetric and asymmetric stretching vibrations of the CH_2 group, respectively [26, 27]. The effect of copper on the lipid bands of the wheat leaves is given in Table 5. The area of the 2850 cm^{-1} band decreased by 28.53, 46.13, and 56.53%, while the area of the 2917 cm^{-1} band decreased by 20.62, 35.81, and 46.92%. The curve fitted data revealed that the copper treatments decreased the ratio of area of the CH_2 and CH_3 bands (CH_2/CH_3). The ratio CH_2/CH_3 was calculated as 19.89 for the control seedling, while for the 25, 50, and 75 μM, it was 17.77, 14.39, and 8.89, respectively.

An abiotic or biotic stress, when induced inside plants, influences the normal metabolic processes and hampers the plant growth. Copper is an essential micronutrient and is involved in normal growth and development of the plant as it is a component of many enzymes and proteins that take part in various metabolic pathways [28]. The decrease in the growth and biomass parameters cast light on the growth inhibitory characteristic of copper when present in excess. Heavy metals are potential inhibitors of photosynthesis in plants. The extent of the change depends on the growth stage at which the stress is induced, the type of heavy metal introduced, and the stress duration. Chlorophyll fluorescence has contributed significantly to the study of heavy metal ion stress in plants, providing information on both the mechanistic effect and the extent of damage to the plant [29]. The observed decrease in the intensity and area of the two chlorophyll bands (685 and 730 nm) is an

indicator of a decrease in the amount of chlorophyll, while the observed increase in the value of fluorescence intensity ratio of I_{685}/I_{730} implies a decline in the photosynthetic rate of the plant. The effect of copper on the photosynthetic apparatus of plants is reflected in its toxic effect on the primary reaction center of the photosystem II (PS II), which is more susceptible to toxicity than PS I [30, 31]. Both donor and acceptor sides of PS II have been proposed as copper inhibitory sites [32]. Higher concentrations of copper have been reported to cause damage to the proteins of the oxygen-evolving complex at the donor and acceptor sites of PS II, the Q_B binding site, and Pheo-Fe-Q_A [33], resulting in a reduction in the quantum yield of PS II [34]. Since copper is known to cause structural alterations, therefore the decrease in the photochemical activity is followed by the damage in the thlakoid membrane [35].

In response to stress conditions, plants activate their defense mechanism such as the accumulation of metabolic fluxes, activation of the antioxidant defense system, and synthesis of amino acids and proteins [36]. An increase was observed in the amide II and amide I content in the leaves of the plants exposed to copper, which indicates the protective strategy of the plant towards copper stress. Exposure of copper results in the accumulation of free amino acids like histidine, proline, and cystein in the plant tissues [37]. The decrease in the area of lipid bands was evident in the leaves exposed to copper. The decrease in the lipid content of the plant in response to heavy metals is due to the oxidative damage caused by free radicals, which are formed due to heavy metal interaction. In the higher plants, the heavy-metal interaction results in the generation of the superoxide radical ($O_2^{\bullet -}$), hydrogen peroxide (H_2O_2), hydroxyl radical (HO•), and singlet oxygen ($^1O_2$), collectively called reactive oxygen species (ROS), and cause oxidative stress. The generated ROS can rapidly attack biomolecules like nucleic acids, proteins, lipids, and amino acids, leading to metabolic dysfunction within the plants [38]. The decrease in the lipid content indicated by the decrease in the area of CH_2 bands throws light on the lipid damage caused by the oxidative stress of copper within the leaves. The decrease in the CH_2/CH_3 ratio is an indicator of disordering of lipids and reflects the transformation in conformation of lipid tails hydrofobic region. The decreased CH_2/CH_3 ratio is also an indicator of the higher fatty acid saturation. The increasing saturation of the fatty acid suggests that the lipid in the seedlings is more susceptible to oxidative damage. Studies have indicated that copper decreases the neutral lipids and total lipid content. This decrease is seen in the lipid content of membranes of organelles such as chloroplast [39]. Copper is also reported to increase lipoxygenase activity and catalyzes lipid peroxidation of unsaturated fatty acids. As a result of the peroxidation reaction, various free radicals are formed, leading to membrane structure disorganization [40]. In addition to amide I, amide II, and lipid content, changes were also observed in the cell wall polysaccharides of the leaves of maize plants. The area of the cellulose bands at 1160 and 1315 cm^{-1} decreased in the leaves exposed to copper. The area of the pectin bands at 1107, 1368, and 1443 cm^{-1} was observed to inrease in the leaves of the seedlings exposed to copper. The cell wall of the plants acts as a physical barrier and restricts the entry of heavy metals into the protoplast of the cells [41]. The polysaccharides, amino acids, and phenolics of the plants play an important role in sequestering and binding heavy metals and making them metabolically inactive [42]. Functional groups like –COOH, –OH, and –SH present on the polysaccharides of the plant cell wall are able to bind divalent and trivalent metal cations [43]. Polysaccharides rich in carboxyl-group such as pectins are synthesized in the Golgi apparatus and secreted in the extracellular region, where they are methyl esterified. The methyl-esterified pectins affect the metal binding process [43]. Analyses of the infrared bands at 1425 and 1480 cm^{-1} pertaining to lignin showed an increase in their band area. The band at 1480 cm^{-1} was absent in the leaves of the control plants. Lignin is a complex component of the cell wall, which is made up of phenolic heteropolymers and is essential for the plant structure formation and defense. It is observed that copper has a positive effect on the synthesis of lignin. Copper is known to increase the activity of peroxidase (PRX) and laccases enzymes which are involved in the polymerization of monolignol precursors of lignin [44]. The observed increase in the pectin and lignin fraction in response to copper can be regarded as a defense strategy of plants towards copper.

Conclusions. This study shows the toxic response of copper as reflected in the reduction in the growth parameters and photosynthetic pigments, as well as alterations in the biochemical content of the maize seedlings. LIF and UV-Vis measurements reveal that treatment with copper decreases the chlorophyll content of the leaves of maize seedlings, while ATR-FTIR measurements show that copper treatment increases the amount of pectin, lignin, amino acids, and proteins and decreases the cellulose and lipid content in the leaves of maize seedlings. This study shows the potential of spectroscopic techniques in studying the physiological status of plants in response to the stress of a heavy metal like copper. Being noninvasive and a rapid probe, chlorophyll fluorescence and ATR-FTIR can be used for the simultaneous investigation of alterations in biochemical constituents and the resulting physiological response due to the changing environment within the biological specimen without any sample preparation.

Acknowledgments. The authors are thankful to Prof. M.M. Joshi and Prof. R. Gopal, former Head, Department of Physics, University of Allahabad, Allahabad for their keen interest in this problem and to UGC, New Delhi for providing

financial assistance for creating the ATR-FTIR facility under the UGC–CAS program at the Department of Physics, University of Allahabad, Allahabad. One of us (Sweta Sharma) is also thankful to UGC, New Delhi for financial assistance in form of SRF (NET).

REFERENCES

1. J. J. Liu, Z. Wei, and J. H. Li, *Bot. Stud.*, **55** (2014); DOI: 10.1186/s40529-014-0047-5.
2. S. Doncheva, Z. Stoyanova, K. Georgieva, D. Nedeva, R. Dikova, G. Zehirov, and A. Nikolova. *J. Plant Nutr. Soil Sci*., **169**, 247–254 (2014).
3. B. Printz, S. Lutts, J. Hausman, and K. Sergeant, *Front. Plant Sci*., **7** (2016); DOI: 10.3389/fpls.2016.00601.
4. K. Drzewiecka, M. Mleczek, M. Gąsecka, Z. Magdziak, A. Budka, T. Chadzinikolau, Z. Kaczmarek, and P. Goliński, *J. Plant Physiol*., **216**, 125–134 (2017).
5. A. S. Badr, G. Patricia, V. D. Florence, T. M-Laure, E. Daniel, and B. Pierre-Marie, *Plant Sci*., **166**, 1213–1218 (2004).
6. Y. Xu, W, Yu, Q. Ma, H. Zhou, and C. Jiang, *Ecotoxicol. Environ. Saf*., **142**, 250–256 (2017).
7. Z. T. Xiong, C. Liu, and B. Geng, *Rupr. Ecotoxicol. Environ. Saf*., **64**, 273–280 (2006).
8. S. Akhtar, A. Shoaib, N. Akhtar, and R. Mehmood, *J. Anim. Plant Sci*., **26**, 1339–1345 (2016)
9. K. Możdżeń, T. Wanic, G. Rut, T. Łaciak, and A. Rzepka, *Photosynthetica*, **55**, 193–200 (2017).
10. S. Khatuna, M. B. Ali, E. J. Hahna, and K. Y. Paeka, *Environ. Exp. Bot*., **64**, 279–285 (2008).
11. Y. V. Ivanov, A. V. Kartashov, A. I. Ivanova, Y. V. Savochkin, and V. V. Kuznetsov, *Environ. Sci. Pollut. Res*., **23**, 17332–17344 (2016).
12. R. Gopal, K. B. Mishra, M. Zeeshan, S. M. Prasad, and M. M. Joshi, *Curr. Sci. India*, **83**, 880–884 (2002).
13. S. Sharma and K. N. Uttam, *Spectrosc. Lett*., **49**, 520–528 (2016).
14. S. Sharma and K. N. Uttam, *Vib. Spectrosc*., **92**, 135–150 (2017).
15. S. Sharma, S. Srivastava, R. Singh, and K. N. Uttam, *Spectrosc. Lett*., **50**, 115–123 (2017).
16. H. K. Lichtenthaler, *Method Enzymol*., **148**, 350–382 (1987).
17. A. Barth, *Prog. Biophys. Mol. Biol*., **74**, 141–173 (2000).
18. P. Robert, M. Marquis, C. Barron, F. Guillon, and L. Saulnier, *J. Agric. Food Chem*., **53**, 7014−7018 (2005).
19. H. Schulz and M. Baranska, *Vib. Spectrosc*., **43**, 13–25 (2007).
20. A. Alonso-Simon, A. E. Encina, P. Garcıa-Angulo, J. M. Alvarez, and J. L. Acebes, *Plant Sci*., **167**, 1273–1281 (2004).
21. N. Labbé, T. G. Rials, S. S. Kelley, Z. M. Cheng, J. Y. Kim, and Y. Li, *Wood Sci. Technol*., **39**, 61–76 (2005).
22. A. Barth, *Biochim. Biophys. Acta*, **1767**, 1073–1101 (2007).
23. K. S. Bandekar, *J. Adv. Protein Chem*., **38**, 181−364 (1986).
24. J. C. Fernandes, P. Garcia-Angulo, L. F. Goulao, J. L. Acebes, and S. Amancio, *Plant Sci*., **205**, 111–120 (2013).
25. J. Yang and H. E. Yen, *Plant Physiol*., **130**, 1032–1042 (2002).
26. J. Heredia-Guerrero, J. Benítez, E. Domínguez, I. Bayer, R. Cingolani, A. Athanassiou, and A. Heredia, *Front. Plant Sci*., **5** (2014); DOI: 10.3389/fpls.2014.00305.
27. R. Lahlali, Y. Jiang, S. Kumar, C. Karunakaran, X. Liu, F. Borondics, E. Hallin, and R. Bueckert, *Front. Plant Sci*., **5** (2004); DOI: 10.3389/fpls.2014.00747.
28. Z. Li, L. Wu, P. Hu, Y. Luo, and P. Christie, *J. Hazard. Mater*., **261**, 332–341 (2003).
29. H. K. Lichtenthaler and U. Rinderle. *C. R. C. Crit. Rev. Anal. Chem.*, **19**, sup. 1, S29–S85 (1988); DOI: 10.1080/15476510.1988.10401466.
30. D. Tanyolac, Y. Ekmekc, and S. Unalan, *Chemosphere*, **67**, 89–98 (2007).
31. M. Bernal, M. Roncel, J. M. Ortega, R. Picorel, and I. Yruela, *Physiol. Plant*., **120**, 686–694 (2004).
32. E. Patsikka, M. Kairavuo, F. Sersen, E. M. Aro, and E. Tyystjarvi, *Plant Physiol*., **129**, 1359–1367 (2002).
33. A. Vassilev, F. Lidon, J. C. Ramalho, C. Do, M. Matos, and G. Da, *J. Central Eur. Agric*., **4**, 225–236 (2003).
34. W. Maksymiec and T. Baszynsi, *J. Plant Physiol*., **149**, 196–200 (1996).
35. F. Monnet, N. Vailant, P. Vernay, A. Coudret, H. Sallanon, and A. Hitmi, *J. Plant Physiol*., **158**, 1137–1144 (2001).
36. H. K. Lichtenthaler, *J. Plant Physiol*., **148**, 4–14 (1996).
37. B. Nedjimi and Y. Daoud, *Funct. Ecol. Plants*, **204**, 316–324 (2009).
38. J. E. J. Weckx and H. M. M. Clijsters, *Physiol. Plant*., **96**, 506–512 (1996).
39. O. Quariti, N. Boussama, M. Zarrouk, A. Cherif, and M. H. Ghorbal, *Phytochemistry*, **45**, 1343–1350 (1997).

40. *Ecological Responses to Environment Stresses*, Kluwer Academic, Netherlands, pp. 22–30 (1981).
41. M. Krzeslowska, *Acta Physiol. Plant*., **33**, 35–51 (2011).
42. M. Ovečka and T. Takáč, *Biotechnol. Adv*., **32**, 73–86 (2014).
43. L. Parrotta, G. Guerriero, K. Sergeant, G. Cai, and J. Hausman. *Front. Plant Sci*., **6** (2015); DOI: 10.3389/fpls.2015.00133.
44. C. C. Lin, L. M. Chen, and Z. H. Liu, *Plant Sci*., **168**, 855–861 (2005).